The University of
Nottingham

UNITED KINGDOM · CHINA · MALAYSIA

Samms, Ricardo J. and Lewis, Jo E. and Lory, Alex and Fowler, Maxine J. and Cooper, Scott and Warner, Amy and Emmerson, Paul and Adams, Andrew C. and Luckett, Jeni C. and Perkins, Alan C. and Wilson, Dana and Barrett, Perry and Tsintzas, Kostas and Ebling, Francis J.P. (2015) Antibody-mediated inhibition of the FGFR1c isoform induces a catabolic lean state in Siberian hamsters. Current Biology, 25 (22). pp. 2997-3003. ISSN 1879-0445

Access from the University of Nottingham repository:
http://eprints.nottingham.ac.uk/34253/1/CBpaper-repository.pdf

Antibody mediated inhibition of the FGFR1c isoform induces a catabolic lean state in Siberian hamsters

Ricardo J Samms[1,2], Jo E Lewis[1], Alex Lory[1], Maxine J Fowler[1], Scott Cooper[1], Amy Warner[1], Paul Emmerson[2], Andrew C Adams[2], Jeni C Luckett[3], Alan C Perkins[3], Dana Wilson[4], Perry Barrett[4], Kostas Tsintzas[1], Francis J P Ebling[1]

[1]School of Life Sciences, University of Nottingham Medical School, Queen's Medical Centre, Nottingham NG7 2UH, UK.

[2]Lilly Research Laboratories, Indianapolis, USA.

[3]School of Medicine, University of Nottingham Medical School, Queen's Medical Centre, Nottingham NG7 2UH, UK.

[4]Rowett Institute for Nutrition and Health, University of Aberdeen, Greenburn Road, Aberdeen AB21 9SB, UK.

Running title: FGFR1c, tanycytes and appetite

Email correspondence to: fran.ebling@nottingham.ac.uk
School of Life Sciences
University of Nottingham Medical School
Queen's Medical Centre
Nottingham
NG7 2UH   UK

tel: +44 115 823 0164   fax: +44 115 823 0142

Word count: Summary: 248   Results/Discussion and Conclusions: 2520

Figures: 4   Supplemental Figures: 4

Summary

Hypothalamic tanycytes are considered to function as sensors of peripheral metabolism [1]. To facilitate this role they express a wide range of receptors, including fibroblast growth factor receptor 1 (FGFR1). Using a monoclonal antibody (IMC-H7) that selectively antagonizes the FGFR1c isoform [2], we investigated possible actions of FGFR1c in a natural animal model of adiposity, the Siberian hamster. Infusion of IMC-H7 into the third ventricle suppressed appetite and increased energy expenditure. Likewise, peripheral treatment with IMC-H7 decreased appetite and body weight, and increased energy expenditure and fat oxidation. A greater reduction in body weight and caloric intake was observed in response to IMC-H7 during the long-day fat state as compared to the short-day lean state. This enhanced response to IMC-H7 was also observed in calorically-restricted hamsters maintained in long days, suggesting that it is the central photoperiodic state rather than the peripheral adiposity that determines the response to FGFR1c antagonism. Hypothalamic thyroid hormone availability is controlled by deiodinase enzymes (DIO2 and DIO3) expressed in tanycytes, and is the key regulator of seasonal cycles of energy balance [3, 4]. Therefore, we determined the effect of IMC-H7 on hypothalamic expression of these deiodinase enzymes. The reductions in food intake and body weight were always associated with decreased expression of DIO2 in the hypothalamic ependymal cell layer containing tanycytes. These data provide further support for the notion the tanycytes are an important component of the mechanism by which the hypothalamus integrates central and peripheral signals to regulate energy intake and expenditure.

Results and Discussion

Expression of FGFR1c in tanycytes

Mammals that have evolved in temperate and polar environments generally display profound seasonal cycles in energy balance comprising changes in appetite, energy expenditure and fat deposition [5]. Analysis of hypothalamic function in seasonal mammals is a strategy to identify novel pharmacological targets for the treatment of obesity and its comorbidities [4, 6]. Recently, it has become clear that hypothalamic tanycytes play a pivotal role in generating seasonal cycles. Annual changes in photoperiod regulate many genes in the ependymal cell layer that contains the tanycyte cell soma, including nestin, GPR50, and those encoding processing enzymes and transporters for thyroid hormone and retinoic acid [7-9]. *In situ* hybridization revealed a high level of expression of FGFR1c in this cell layer (Figure 1A, Figure S1), consistent with previous quantitative PCR studies in the mouse [10]. FGFR1c is a member of the tyrosine kinase FGF receptor family that are thought to play diverse roles in the development, growth and regeneration of tissue [11]. Antibody-mediated targeting of FGFR1c reduces body weight, fat mass and insulin resistance in animal models of obesity and type II diabetes [2, 12, 13]. The aim of the current studies was to investigate the role of FGFR1c in the regulation of body weight, food intake and metabolism using a monoclonal antibody antagonist (IMC-H7) that selectively targets the FGFR1c isoform [2].

Although IMC-H7 was shown to bind specifically in the mediobasal hypothalamus of mice [2], and was originally characterized as an antagonist on the basis of its ability to block binding of FGF2 to FGFR1c expressed in a myoblast cell line [2], we confirmed its ability to target tanycytes by testing its activity in primary cultures [14]. Ligand-mediated activation of tyrosine kinase FGFR is characterized by induction of MAP kinase (ERK1/2) and Akt signalling, so we determined its ability to inhibit signalling of a canonical FGFR1 ligand, FGF2. FGF2 (10nM) treatment increased the phosphorylation of ERK1/2 and Akt in rat primary tanycytes (Figure 1B-E). IMC-H7 itself did not increase phosphorylation of ERK1/2 or Akt either acutely or following a 1h incubation period (Figure 1B-E), however, IMC-H7 was able to block FGF2-mediated phosphorylation of ERK1/2 and Akt when pre-incubated with the primary cell cultures for 1h prior to adding FGF2 (Figure 1B-E). Our previous immunohistochemical and PCR analyses of the primary cultures derived from microdissected ependymal walls suggests they are highly enriched for tanycyte markers (vimentin) but not for markers of astrocytes (GFAP) or neighbouring pars tuberalis (TSHβ) [14]. We therefore infer that IMC-H7 is exerting its antagonistic action via binding to receptors on tanycytes.

We determined the effect of FGFR1c blockade *in vivo* by infusing 0.5μg IMC-H7 via an intracerebroventricular cannula. Such treatment caused a significant reduction in body weight that

had not returned to baseline by 96h after treatment (Figure 1F). This reflected a significant reduction in food intake over the first 48h after infusion (Figure 1G) that did not return to baseline until 72h after infusion. It also caused an increase in energy expenditure from 24-72h post infusion (Figure 1H) that was associated with a trend ($P=0.07$) towards increased fat oxidation during the dark phase (Figure 1I). Although fasting plasma leptin concentrations were not affected 96h after IMC-H7 administration (Figure 1J), insulin concentrations were decreased (Figure 1K).

Systemic FGFR1c blockade mimics central responses

Tanycytes form a structural component of the blood-brain barrier in that their end feet appose endothelial cells surrounding capillaries in the median eminence [15]. They express a wide range of hormone receptors and nutrient sensors that underpin their role in mediating metabolic signalling to the hypothalamus [16, 17]. The objective of this study was to compare peripheral effects of FGFR1c blockade to the central effects. There was a dose-dependent decrease in body weight following systemic IMC-H7 treatment (Figure 2A). This persisted for the first 5-6 days after infusion in hamsters treated with the highest dose (3mg/kg) of IMC-H7. This long-term action is consistent with the 3-5 day half-life of a similar monoclonal antibody antagonist, as previously estimated in mice [2]. The weight loss reflected a substantial suppression of food intake (Figure 2B), but also an increase in energy expenditure in hamsters treated with the highest dose of IMC-H7, as assessed on day 6-7 after the start of treatment (Figure 2C). At this point fat oxidation was significantly increased (Figure 2D), and carbohydrate oxidation decreased (Figure 2E). Analysis of body composition using computed tomography revealed that the loss of body weight induced by FGFR1c blockade reflected a significant reduction in the volume of adipose tissue (Figure 2F, G).

Photoperiodic regulation of responses to FGFR1c blockade

We repeated the dose-response study in hamsters acclimatised to short photoperiods (SD) for 12 weeks to induce a lean hypophagic state, and noted that the responses to IMC-H7 were attenuated (Figure S2). We therefore compared directly responses to IMC-H7 in age-matched hamsters previously exposed to long or short photoperiods (Figures 2H-J, 3). Treatment with IMC-H7 at a dose of 3 mg/kg decreased body weight in hamsters maintained in both photoperiods (Figure 3A, B), but again the effects of IMC-H7 were more pronounced in hamsters maintained in their LD fat state: body weight was reduced by ~12% in hamsters in LD compared to ~7% reduction in hamsters maintained in SD (Figure 3A, B). Similarly, there were clear suppressive effects of IMC-H7 on food intake throughout the treatment period in hamsters maintained in LD (Figure 3C) and on days 2 and 3 in hamsters in SD (Figure 3D). Treatment with IMC-H7 significantly increased daily energy expenditure in animals maintained in LD (Figure 3E). Importantly, similar to the pilot dose-response studies, treatment with IMC-H7 did not significantly affect energy expenditure in hamsters in SD (Figure 3F). Forty-eight hours after IMC-H7 treatment began there was a clear switch in metabolic fuel utilization, that is, a significant increase in fat oxidation (Figure 3G, H) and a decrease in carbohydrate oxidation (Figure 3I, J). This occurred in hamsters treated with IMC-H7 maintained in both photoperiods, but again the magnitudes of these responses were reduced in the SD-exposed hamsters (Figure 3G-J). Fasting blood glucose concentrations were not affected at the end of the study (Figure 2H), but fasting insulin (Figure 2I) and leptin (Figure 2J) concentrations were significantly lower in hamsters in LD. The insulin response mirrored that following intracerebroventricular administration of IMC-H7 (Figure 1K). Insulin concentrations were not significantly affected by FGFR1c antagonism in hamsters in SD (Figure 2I), and circulating leptin concentrations were close to the limit of detection in all hamsters in SD, so no effect was detected (Figure 2J). Clearly systemic treatment with IMC-H7 has potent effects on food intake and body weight that resemble the effects of central treatment, so these observations are consistent with the view that peripheral treatment with IMC-H7 may also be targeting central FGFR1c. The suppression of appetite is consistent with a central action, and it is noticeable that the decrease in circulating leptin observed after systemic administration of IMC-H7 is not sufficient to promote a compensatory hyperphagic response.

We found no evidence of altered FGFR1c gene expression in the ependymal cell layer of hamsters in LD and SD (Figure S1) that might explain the differential responses to FGFR1c antagonism. We considered that these differential responses to IMC-H7 in LD and SD could therefore either be due to the reduced peripheral adiposity of hamsters in the SD state (e.g. epididymal fat reduction of ~20%), or could be a reflection of the underlying photoperiodically-regulated central state. To distinguish these two possibilities, we tested the effects of IMC-H7 in hamsters in which peripheral fat loss was caused by caloric restriction for 5 weeks rather than by exposure to a SD photoperiod (Figure S3). Clear catabolic responses to IMC-H7 were observed that resembled those previously observed in fat hamsters in LD (Figure S3), suggesting that central photoperiodic state rather than peripheral adiposity was the key factor determining the response to FGFR1c blockade.

Hypothalamic gene expression after FGFR1c blockade

To understand better how blockade of FGFR1c might affect tanycyte function, we used *in situ* hybridization to assess expression of DIO2 and DIO3 after IMC-H7 treatment. These genes are pivotal in the seasonal regulation of energy balance by virtue of their regulation of the local availability of tri-iodothyronine [18]. As previously reported, there was clear mRNA expression for both DIO2 and DIO3 in the ependymal layer surrounding the ventral third ventricle, and short day exposure reduced DIO2 mRNA expression by 3-fold but hugely increased DIO3 expression (Figure 4A-D). Importantly, treatment of hamsters in LD with IMC-H7 resulted in a 2-fold decrease in DIO2 mRNA expression ($P<0.001$) when compared to vehicle-treated hamsters (Figure 4A, B). There were no effects of treatment on DIO3 mRNA expression in animals maintained in either LD or SD (Figure 4A-D). This clear decrease in DIO2 expression in the ependymal cell layer was also observed in the study where previously food-restricted hamsters in LD were treated with IMC-H7 (Figure 4E, F). The decrease in DIO2 expression would be expected to cause a reduction in local tri-iodothyronine (T3) availability in the surrounding hypothalamus [19]. We have previously observed that local delivery of T3 into the hypothalamus via slow-release microimplants causes increased food intake, reduced energy expenditure, and thus increased body weight in hamsters [20], so the reverse responses observed after IMC-H7 treatment in the current study are consistent with the reduction in DIO2 expression and in T3 availability.

We also analysed a number of other genes in the hypothalamus implicated in the control of food intake and energy expenditure. NPY, AgRP, POMC and CART mRNA expression were highly localized to the arcuate nucleus (ARC) and TRH and CRH mRNA were highly expressed in the PVN, but there were no effects of photoperiod or IMC-H7 treatment on any of these known homeostatic regulators of energy balance (Figure 4H, Figure S4). There was a significant increase in somatostatin (SRIF) mRNA abundance in the ARC following IMC-H7 treatment though the magnitude of increase was not as great as that induced by exposure to SD (Figure S4). The SD-induced increase in SRIF has been observed previously in hamsters [21, 22], and is likely to contribute to the development of the SD phenotype [23], so the increase in SRIF may be one of the downstream mediators of the catabolic response resulting from FGFR1c blockade. Collectively, these observations indicate that the effects of IMC-H7 on DIO2 expression are very specific to the ependymal cell layer, consistent with the view that FGFR1c signalling is specific to tanycytes. Given the previous evidence that photoperiod regulates deiodinase gene expression in tanycytes, we should view these cells as a locus that integrates both photoperiodic and other nutritional and metabolic signals to regulate energy balance.

Conclusions

Our observations in hamsters concur with previous studies in mice, rats and rhesus monkeys that antibody-mediated inhibition of FGFR1c decreases food intake and body weight [2], and extend our understanding in two important directions. First, they provide evidence that the effects of IMC-H7 may be mediated centrally via regulation of tanycyte function. FGFR signalling in primary cultures of tanycytes was blocked by IMC-H7, and *in vivo* treatment with IMC-H7 significantly reduced DIO2 expression in the ependymal cell layer, whereas gene expression encoding homeostatic peptides (NPY, AgRP, POMC, CART [24]) was unaffected. It has been previously suggested that the effects of

IMC-H7 on food intake are likely to be central on the grounds that a similar antibody (IMC-A1) bound to the median eminence/mediobasal hypothalamus in mice [2]. We found that ICV infusion of IMC-H7 directly into the hypothalamic third ventricle significantly decreased body weight at an approximately 200-fold lower dose than that required via peripheral administration, again consistent with a local site of action within the hypothalamus.

Second, we found that the effect of FGFR1c inhibition on caloric intake was greater in hamsters in the LD fat state when compared to those in the SD lean state, suggesting that activity of the FGFR1c system might vary as a function of either adiposity or photoperiod. One interpretation of these findings might be that adipose tissue is a direct target of IMC-H7, thus fat hamsters in LD would show an enhanced response. White adipose tissue expresses FGFR1c, and targeted knockout of this receptor from adipocytes greatly reduces the responsiveness of mice to FGF21, a ligand for FGFR1c [25]. However, the effects of FGFR1c blockade in calorically-restricted hamsters in LD whose fat stores had been depleted to levels characteristic of SD hamsters were comparable to those in hamsters in LD on *ad libitum* diet. This suggests that photoperiod rather than peripheral adiposity is the more important determinant of the effects of FGFR1c blockade, so it is changes in central state that determine the response to IMC-H7, that is, the primary actions of IMC-H7 are central rather than peripheral. This interpretation is reinforced by the striking effects of FGFR1c blockade on DIO2 gene expression in the hypothalamus, as changes in expression of hypothalamic deiodinases are a key mechanism underlying photoperiodic regulation of cycles of appetite and metabolism [4]. Although the predominant form of circulating thyroid hormone is the relatively inactive precursor thyroxine (T4), it is the tanycyte-specific expression of the MCT8 transporter and of deiodinase enzymes that regulate local bioactive T3 availability in the hypothalamus [26, 27]. The reduction in food intake that occurs when switching Siberian hamsters from LD to SD is primarily associated with the reduction in hypothalamic thyroid hormone availability resulting from decreased expression of DIO2 and a reciprocal increase in DIO3 expression in the ependymal tanycyte layer [7, 20]. In the current study, the IMC-H7-mediated reduction in daily food intake was associated with a significant decrease in DIO2 mRNA expression in the ependymal tanycyte layer when hamsters were housed in LD, but not in SD when DIO2 expression was already reduced. Likewise, there was a significant decrease in DIO2 mRNA expression in the ependymal tanycyte layer of the mediobasal hypothalamus in food-restricted animals treated with IMC-H7 when compared to vehicle. Thus, antibody-mediated inhibition of food intake is associated with a reduction in DIO2 mRNA expression in the tanycyte layer of the mediobasal hypothalamus regardless of the prevailing adiposity. Furthermore, it seems that the blunted responses to IMC-H7 treatment in animals maintained in SD may be due to the already reduced mRNA expression of DIO2 in the mediobasal hypothalamus. The mechanism of action of thyroid hormone on appetite remains to be determined, but the increased expression of SRIF may be one potential pathway. There is also robust evidence in mice that fasting induces DIO2 expression and increases T3 concentrations in the mediobasal hypothalamus, and that the glial elements expressing DIO2 are closely apposed to NPY/AgRP neurons in the ARC [28]. The increase in T3 was demonstrated to promote mitochondrial uncoupling and increase neuronal excitability in these orexigenic NPY/AgRP neurons via an uncoupling protein 2 mechanism [28]. Conversely, a decrease in DIO2 expression and therefore T3 availability might be expected to reduce NPY/AgRP activity, which would then contribute to the decreased food intake we observed after FGFR1c blockade. Collectively, we consider that our *in vitro* and *in vivo* observations provide evidence that FGFR1c signalling in tanycytes and subsequent regulation of local thyroid hormone availability is a physiologically important mechanism in the regulation of appetite.

Experimental Procedures
Supplemental information including detailed experimental procedures and four figures and can be found with this article online at…

(with RJS); RJS, JEL, PE, ACA, KT, FJPE designed the studies; RJS, ACA, PB, KT, FJPE wrote and revised the manuscript.

References

1.   Bolborea, M., and Dale, N. (2013). Hypothalamic tanycytes: potential roles in the control of feeding and energy balance. Trends in Neurosciences *36*, 91-100.
2.   Sun, H.D., Malabunga, M., Tonra, J.R., DiRenzo, R., Carrick, F.E., Zheng, H., Berthoud, H.R., McGuinness, O.P., Shen, J., Bohlen, P., et al. (2007). Monoclonal antibody antagonists of hypothalamic FGFR1 cause potent but reversible hypophagia and weight loss in rodents and monkeys. American Journal of Physiology *292*, E964-E976.
3.   Dardente, H., Hazlerigg, D.G., and Ebling, F.J.P. (2014). Thyroid hormone and seasonal rhythmicity. Frontiers in Endocrinology *5*, 19. doi: 10.3389/fendo.2014.00019
4.   Ebling, F.J. (2015). Hypothalamic control of seasonal changes in food intake and body weight. Frontiers in Neuroendocrinology *37*, 97-107.
5.   Hazlerigg, D.G., and Loudon, A.S.I. (2008). Seasonal life timers: new insights into ancient mechanisms. Current Biology *18*, R795-R804.
6.   Ebling, F.J.P. (2014). On the value of seasonal mammals for identifying mechanisms underlying the control of food intake and body weight. Hormones and Behavior *66*, 55-61.
7.   Barrett, P., Ebling, F.J.P., Schuhler, S., Wilson, D., Ross, A.W., Warner, A., Jethwa, P.H., Boelen, A., Visser, T.J., Ozanne, D.M., et al. (2007). Hypothalamic thyroid hormone catabolism acts as a gatekeeper for the seasonal control of body weight and reproduction. Endocrinology *148*, 3608-3617.
8.   Barrett, P., Ivanova, E., Graham, E.S., Ross, A.W., Wilson, D., Ple, H., Mercer, J.G., Ebling, F.J.P., Schuhler, S., Dupre, S.M., et al. (2006). Photoperiodic regulation of GPR50, Nestin and CRBP1 in tanycytes of the third ventricle ependymal layer of the Siberian hamster. Journal of Endocrinology *191*, 687-698.
9.   Hanon, E.A., Lincoln, G.A., Fustin, J.M., Dardente, H., Masson-Pevet, M., Morgan, P.J., and Hazlerigg, D.G. (2008). Ancestral TSH mechanism signals summer in a photoperiodic mammal. Current Biology *18*, 1147-1152.
10.   Fon Tacer, K., Bookout, A.L., Ding, X., Kurosu, H., John, G.B., Wang, L., Goetz, R., Mohammadi, M., Kuro-o, M., Mangelsdorf, D.J., et al. (2010). Research resource: Comprehensive expression atlas of the fibroblast growth factor system in adult mouse. Molecular Endocrinology *24*, 2050-2064.
11.   Beenken, A., and Mohammadi, M. (2009). The FGF family: biology, pathophysiology and therapy. Nature Reviews Drug Discovery *8*, 235-253.
12.   Wu, A.L., Kolumam, G., Stawicki, S., Chen, Y., Li, J., Zavala-Solorio, J., Phamluong, K., Feng, B., Li, L., Marsters, S., et al. (2011). Amelioration of type 2 diabetes by antibody-mediated activation of fibroblast growth factor receptor 1. Science Translational Medicine *3*, 113ra126. doi: 110.1126/scitranslmed.3002669.
13.   Foltz, I.N., Hu, S., King, C., Wu, X., Yang, C., Wang, W., Weiszmann, J., Stevens, J., Chen, J.S., Nuanmanee, N., et al. (2012). Treating Diabetes and Obesity with an FGF21-Mimetic Antibody Activating the ßKlotho/FGFR1c Receptor Complex. Science Translational Medicine *4*, 162ra153. doi: 110.1126/scitranslmed.3004690.

14.   Bolborea, M., Helfer, G., Ebling, F.J., and Barrett, P. (2015). Dual signal transduction pathways activated by TSH receptors in rat primary tanycyte cultures. Journal of Molecular Endocrinology *54*, 241-250.

15.   Rodriguez, E.M., Blazquez, J.L., Pastor, F.E., Pelaez, B., Pena, P., Peruzzo, B., and Amat, P. (2005). Hypothalamic tanycytes: a key component of brain-endocrine interaction. International review of cytology *247*, 89-164.

16.   Langlet, F. (2014). Tanycytes: a gateway to the metabolic hypothalamus. Journal of Neuroendocrinology *25*, 753-760.

17.   Frayling, C., Britton, R., and Dale, N. (2011). ATP-mediated glucosensing by hypothalamic tanycytes. Journal of Physiology *589*, 2275-2286.

18.   Yoshimura, T. (2013). Thyroid hormone and seasonal regulation of reproduction. Frontiers in Neuroendocrinology *34*, 157-166.

19.   Bechtold, D.A., and Loudon, A.S.I. (2007). Hypothalamic thyroid hormones: mediators of seasonal physiology. Endocrinology *148*, 3605-3607.

20.   Murphy, M., Jethwa, P.H., Warner, A., Barrett, P., Nilaweera, K.N., Brameld, J.M., and Ebling, F.J.P. (2012). Effects of manipulating hypothalamic tri-iodothyronine concentrations on seasonal body weight and torpor cycles in Siberian hamsters. Endocrinology *153*, 101-112.

21.   Herwig, A., Petri, I., and Barrett, P. (2012). Hypothalamic gene expression rapidly changes in response to photoperiod in juvenile Siberian hamsters (Phodopus sungorus). Journal of Neuroendocrinology *24*, 991-998.

22.   Herwig, A., de Vries, E.M., Bolborea, M., Wilson, D., Mercer, J.G., Ebling, F.J.P., Morgan, P.J., and Barrett, P. (2013). Hypothalamic ventricular ependymal thyroid hormone deiodinases are an important element of circannual timing in the Siberian hamster (Phodopus sungorus). PLoS One *8*, e62003-doi:62010.61371/journal.pone.0062003.

23.   Dumbell, R.A., Scherbarth, F., Diedrich, V., Schmid, H.A., Steinlechner, S., and Barrett, P. (2015). Somatostatin agonist pasireotide promotes a physiological state resembling short-day acclimation in the photoperiodic male Siberian hamster (Phodopus sungorus). Journal of Neuroendocrinology *27*, 588-599.

24.   Williams, K.W., and Elmquist, J.K. (2012). From neuroanatomy to behavior: central integration of peripheral signals regulating feeding behavior. Nature Neuroscience *15*, 1350-1355.

25.   Adams, A.C., Yang, C., Coskun, T., Cheng, C.C., Gimeno, R.E., Luo, Y., and Kharitonenkov, A. (2013). The breadth of FGF21's metabolic actions are governed by FGFR1 in adipose tissue. Molecular Metabolism *2*, 31-37.

26.   Herwig, A., Wilson, D., Logie, T.J., Boelen, A., Morgan, P.J., Mercer, J.G., and Barrett, P. (2009). Photoperiod and acute energy deficits interact on components of the thyroid hormone system in hypothalamic tanycytes of the Siberian hamster. American Journal of Physiology *296*, R1307-R1315.

27.   Warner, A., and Mittag, J. (2012). Thyroid hormone and the central control of homeostasis. Journal of Molecular Endocrinology *49*, 29-36.

28.   Coppola, A., Liu, Z.W., Andrews, Z., Paradis, E., Roy, M.C., Friedman, J.M., Ricquier, D., Richard, D., Horvath, T.L., and Gao, X.B. (2007). A central thermogenic-like mechanism in feeding regulation: an interplay between arcuate nucleus T3 and UCP2. Cell Metabolism *5*, 21-33.
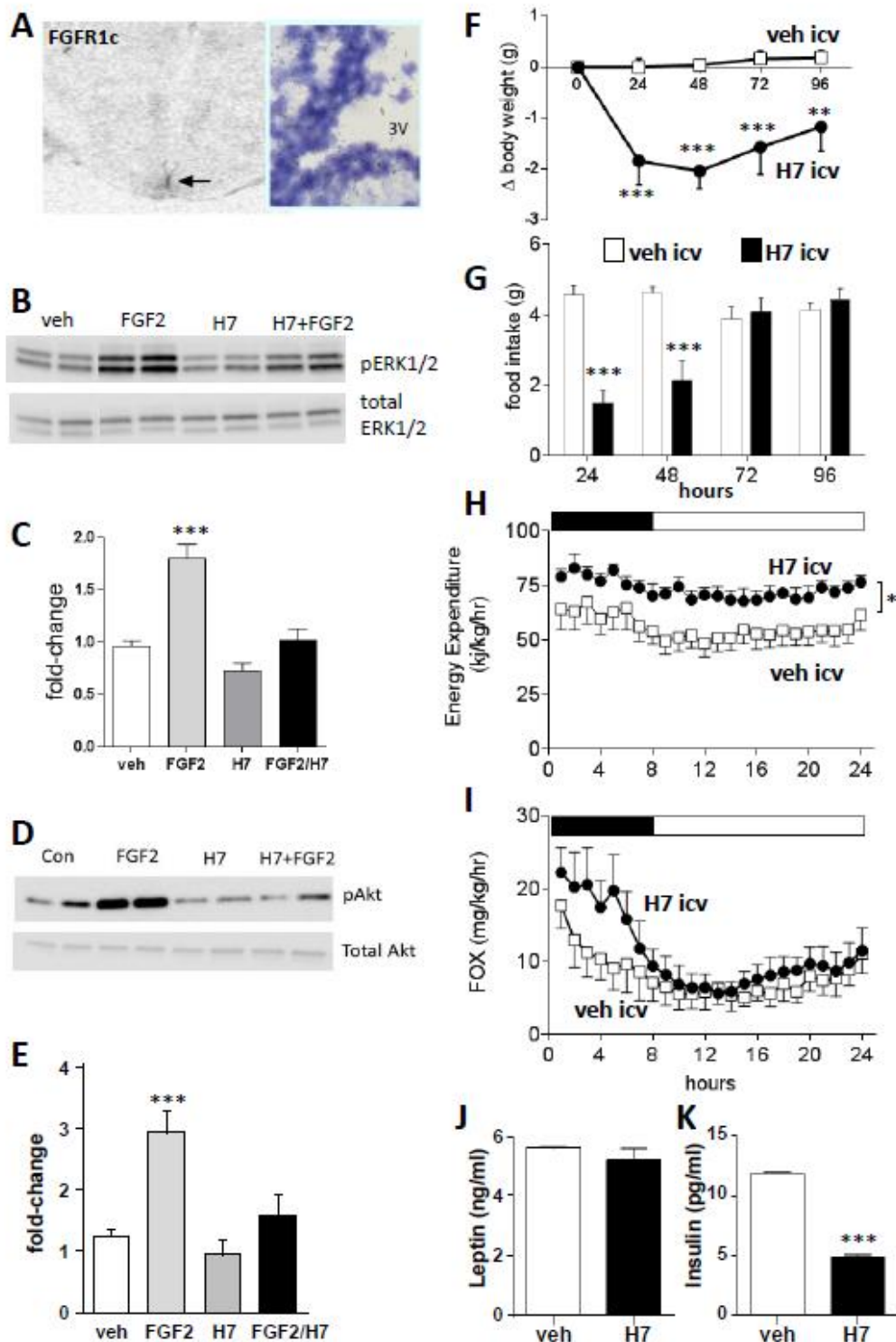
Figure 1

Figure 1. A monoclonal Ab raised against FGFR1c blocks signal transduction in tanycytes and elicits physiological responses *in vivo* after central infusion
A *in situ* hybridization of a ^{35}S labelled probe for FGFR1c on a coronal section through the mediobasal hypothalamus of a Siberian hamster maintained in LD, arrow indicates ependymal region surrounding the third ventricle; emulsion-coated slide showing silver grains arising from hybridization of a FGF1Rc probe (3V = third ventricle). B Western blots showing ERK1/2

8

phosphorylation following treatment with 10nM FGF2, antibody IMC-H7 (H7) or pre-treatment with H7 followed by 10nM FGF2. Each blot is one representative experiment out of three. C mean (±SEM) values, normalized to total ERK1/2, n=6 per treatment, ***p<0.001 vs vehicle. D Western blots showing Akt phosphorylation, samples as for B. E mean (±SEM) values, normalized to total Akt, n=6 per treatment, ***p<0.001 vs vehicle. F changes in body weight in adult male hamsters that received an intracerebroventricular (ICV) infusion of 0.5μg IMC-H7 (n=7) or vehicle (n=8), **p<0.01, ***p<0.001 vs vehicle. G daily food intake in hamsters receiving ICV IMC-H7 or vehicle, ***p<0.001 vs vehicle. H calculated energy expenditure and I fat oxidation (FOX) in vehicle and IMC-H7 treated hamsters from 72-96 hours after the ICV infusion, *p<0.05 vs vehicle. Solid bars (H, I) indicate dark phase. J plasma leptin and K insulin concentrations 96 hours after treatment, ***p<0.001 vs vehicle. See also Figure S1 for analysis of FGFR1 gene expression in LDS vs SD.
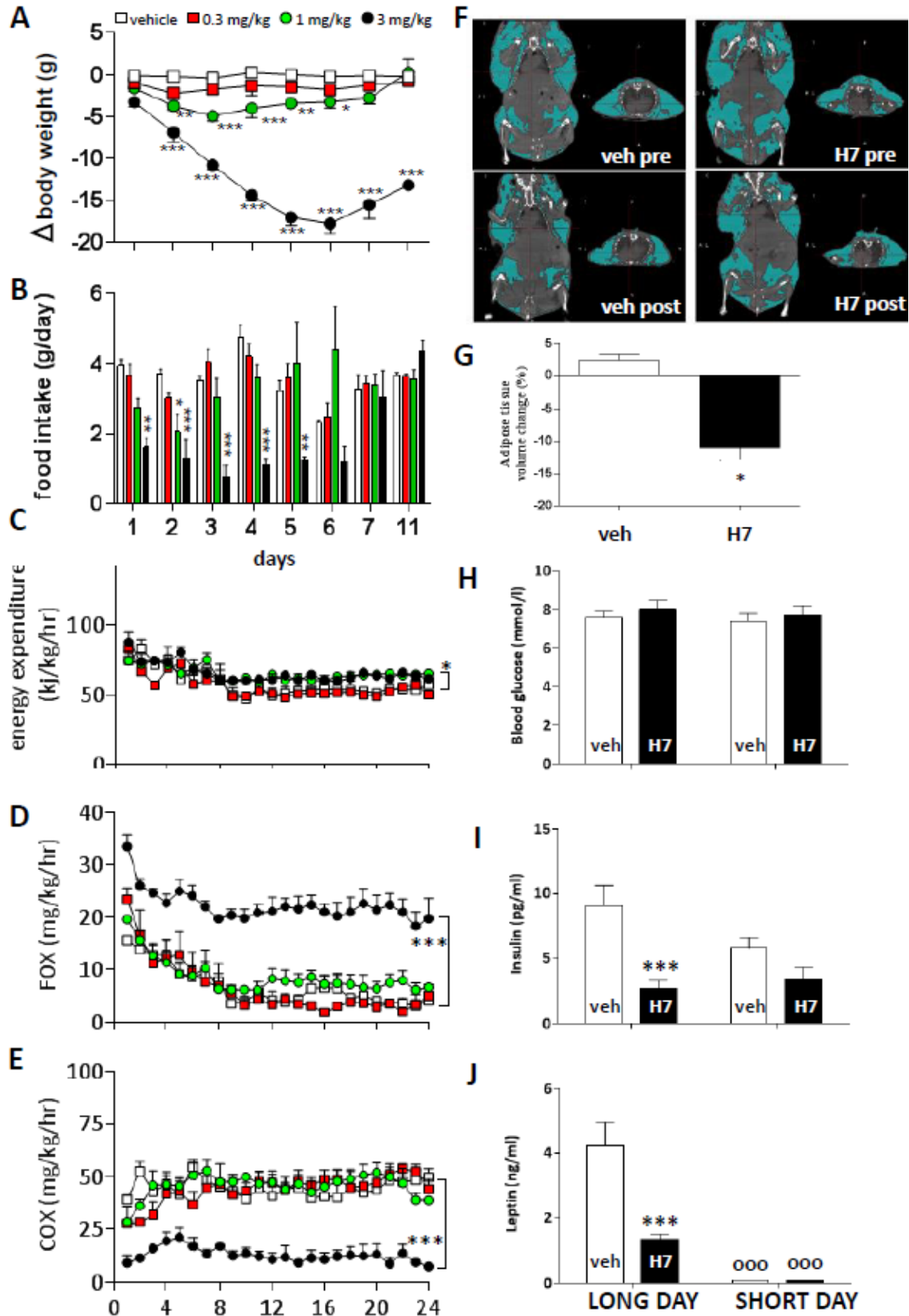
Figure 2

Figure 2. Systemic treatment with a monoclonal Ab raised against FGFR1c increases fat oxidation and promotes weight loss
A changes in body weight and B daily food intake in adult male hamsters in LD treated subcutaneously with vehicle (□) or increasing doses of IMC-H7 (□ 0.3 mg/kg, ● 1.0 mg/kg, ● 3 mg/kg)

10

and monitored for 11 days, values are group mean ± SEM, n=4 per treatment, *p<0.05, **p<0.01 and ***p<0.001 vs vehicle. Hamsters were placed in metabolic cages (CLAMS) 5 days after vehicle or IMC-H7 treatment, values shown are hourly mean ± SEM values calculated for energy expenditure (C), fat oxidation (FOX: D) and carbohydrate oxidation (COX: E) from day 6-7 after treatment; *p<0.05 and ***p<0.001 main effect of treatment vs vehicle. F: representative CT scan images before and 7 days after vehicle or 3 mg/kg IMC-H7 treatment, blue shading indicates values above 200 Hounsfield units. G whole body fat mass derived from microCT, values are group mean (± SEM), n=6 per group, *p<0.05 vs vehicle. Blood glucose (H), insulin (I) and leptin (J) concentrations in age-matched adult male hamsters maintained in long or short days for 12 weeks then treated with vehicle of IMC-H7 (3 mg/kg) for 72 hours, values are group mean (± SEM), n=6-8 per group, ***p<0.001 vs vehicle, °°°p<0.001 vs long day values. See also Figure S2 for effects of IMC-H7 in short days (SD).
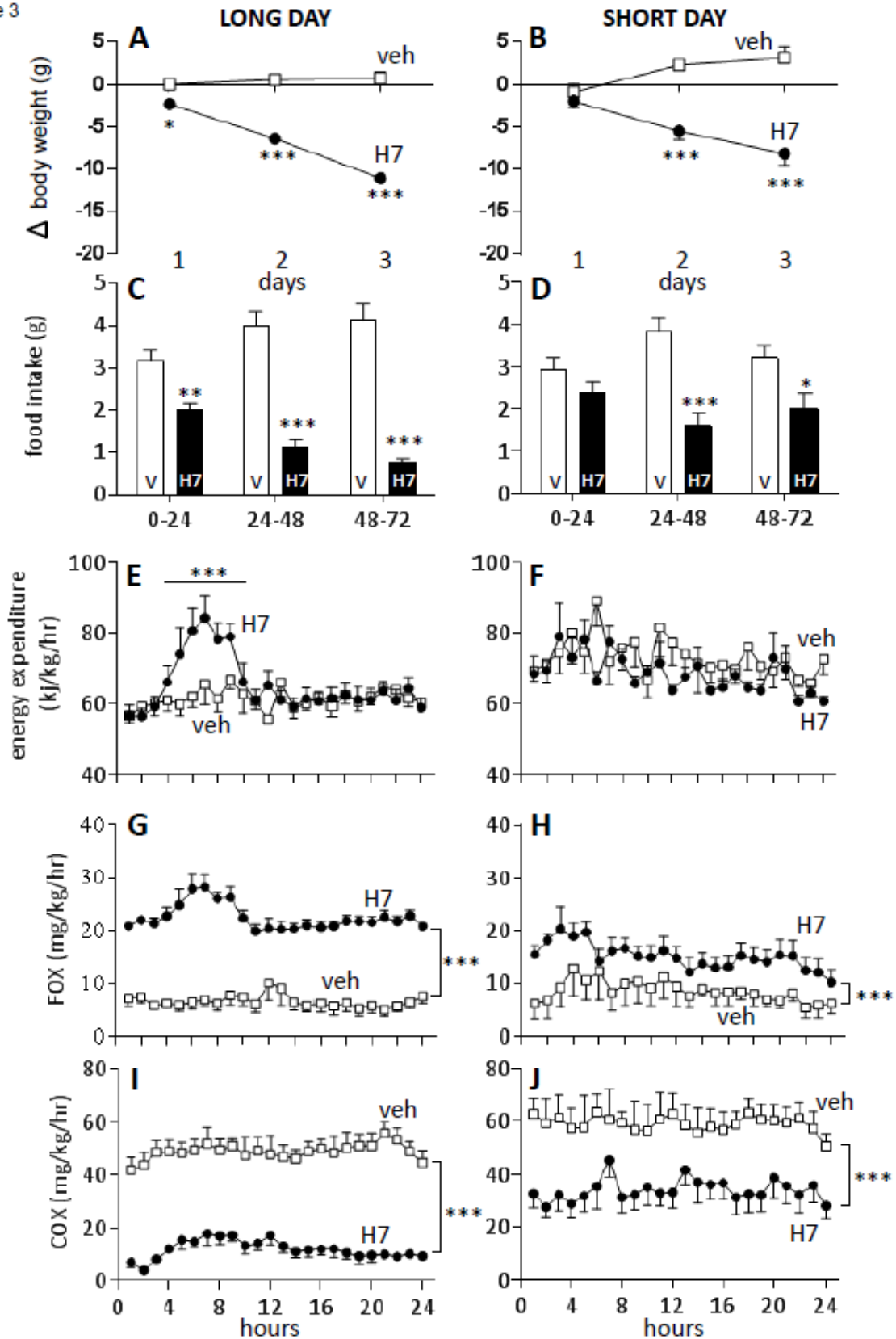
Figure 3. Suppression of food intake and increases in fat oxidation in response to FGFR1c blockade are more pronounced in hamsters in the long day fat state
Upper panels: change in body weight in age-matched adult male hamsters in LD (A) or exposed to 12 weeks of SD (B) treated with vehicle (□) or IMC-H7 (● 3 mg/kg). Corresponding food intake is shown below in panels C (LD) and D (SD). Values are group mean ± SEM, n=6 per treatment, *p<0.05, **p<0.01 and ***p<0.001 vs vehicle. Lower panels: analysis of metabolic cage (CLAMS) data after vehicle (□) or IMC-H7 treatment (● 3 mg/kg). Hourly mean ± SEM values were calculated for energy

expenditure (E LD, F SD), fat oxidation (FOX: G LD, H SD) and carbohydrate oxidation (COX: I LD, J SD), from 48-72 hours after treatment, ***$p<0.001$ main effect of treatment vs vehicle (treatment x time interaction in panel E). See also Figure S3 for effects of IMC-H7 in hamster in LD previously food-restricted to reduce adiposity.
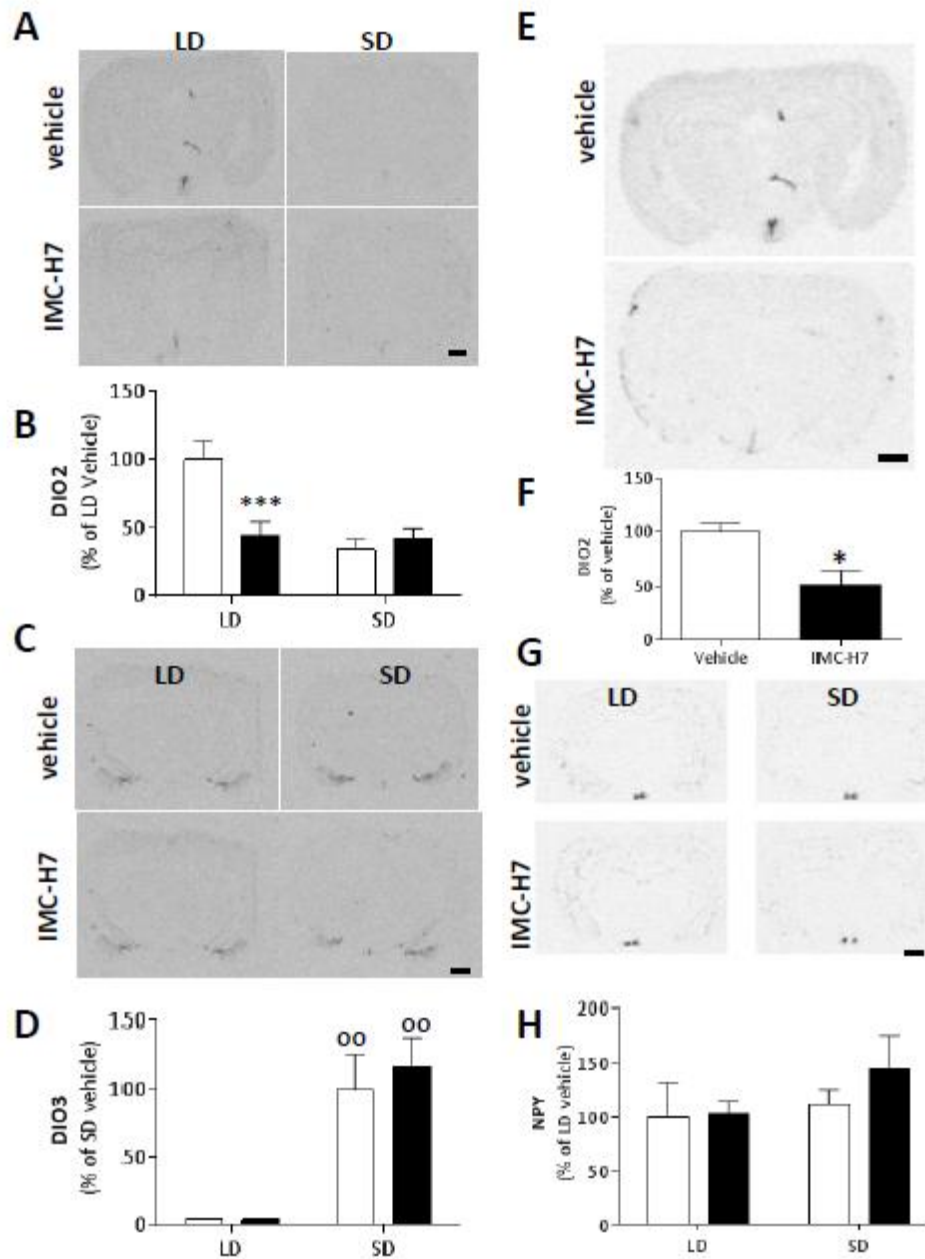
Figure 4

Figure 4. Responses to FGFR1c blockade are associated with suppression of deiodinase 2 gene expression in tanycytes in the hypothalamic ependymal cell layer
Representative autoradiographic film images from adult male hamsters in long days (LD) or short days (LD) revealing DIO2 (A) and DIO3 (C) mRNA distributions and relative density (B DIO2 , D DIO3) of hybridization signal 7 days after treatment with vehicle (□) or 3 mg/kg IMC-H7 (■). Values are group mean ± SEM, n=6 per group, ***p<0.001 vs vehicle, ᵒᵒp<0.01 vs long day values. E autoradiographic film images revealing DIO2 from vehicle and IMC-H7-treated adult male hamsters in LD that had previously been calorically restricted such that their body weight and adiposity was comparable to SD-exposed hamsters. F relative density of hybridization signal around the third

ventricle after 3 days treatment with vehicle (□) or IMC-H7 (■). Values are group mean ± SEM, n=6 per group, *p<0.05 vs vehicle. G representative autoradiographic images and H relative density of signal for NPY mRNA in hamsters in LD or SD, 7 days after treatment with vehicle (□) or 3 mg/kg IMC-H7 (■). Values are group mean ± SEM, n=6 per group. Scale bars in lower right panels are 1000μm. See also Figure S4 for autoradiographic images and density analysis of other hypothalamic genes.

Supplemental Experimental Procedures
Animals
Male Siberian hamsters (*Phodopus sungorus*) were obtained from a breeding colony maintained at the University of Nottingham BioSupport Unit [S1]. Studies followed ARRIVE guidelines [S2], and were carried out in accordance with the UK Animals (Scientific Procedures) Act of 1986 (project licence: PPL 40/3604) and approved by the University of Nottingham Animal Welfare and Ethical Review Board. Hamsters were group housed at approximately 21°C and 40% humidity, and were allowed *ad libitum* access to water and standard laboratory chow comprising of 19% protein, 45% carbohydrate, 9% fat (Teklad 2019, Harlan, UK). Animals were housed from birth in long day conditions (LD) of 16 hours light: 8 hours dark with lights off at 11:00 GMT, short day (SD) exposure comprised 8 hours light: 16 hours dark with lights off maintained at 11:00 GMT.

Effects of IMC-H7 on signal transduction in primary cultures of hypothalamic tanycytes
Primary tanycyte cell cultures were prepared from 8-10 day old Sprague-Dawley rat. Brains were collected and micro-dissected in ice-cold Dulbecco's phosphate buffer saline solution (Sigma Aldrich) using a binocular magnifying microscope After the micro-dissection of the median eminence and the floor of the third ventricle, or small parts of the cortex as a control region, explants were collected in ice-cold Dulbecco's modified Eagle medium (DMEM; Sigma Aldrich). Explants were pooled and dissociated on a 20 μm nylon membrane (Sefar). Cells were cultured in DMEM supplemented with 10% foetal bovine serum (Sigma Aldrich) on 25 cm^2 flasks (Corning Costar or Sigma Aldrich) under humid atmosphere of 5% CO_2-95% air at 37°C. The initial culture medium was changed after 3 or 4 days. These procedures have been described previously [S3, S4].

Effects of central administration of IMC-H7 on body weight, food intake and energy expenditure in the Siberian hamster.
The effects of a single intracerebroventricular (ICV) infusion of IMC-H7 (0.5μg in 1μl) were determined in adult male Siberian hamsters that had been housed in LD since birth. Body weight and food intake were recorded on a weekly basis prior to the start of the experimental period. Hamsters were singly housed for 7 days prior to surgical preparation. Siberian hamsters were anesthetized with isoflurane (1.5%). Analgesia was maintained via sc injection of carprofen (50 mg/kg Rimadyl; Pfizer) administered before surgery and daily afterwards during the recovery period. ICV cannulation and infusion were carried out as previous described [S5]. Following a 7 day recovery period animals received either a single ICV infusion of either saline or IMC-H7 (0.5μg/μl). Body weight and food intake were recorded daily. 48 hours after the infusion, animals were transferred to CLAMS for 48 hours.

Dose-response studies: effect of peripheral administration of IMC-H7 on body weight, food intake and energy expenditure
The effects of IMC-H7 were measured in adult male hamsters that had been housed in LD since birth (n=16). Animals from each photoperiod were divided into one of four dose groups and received a single subcutaneous injection of either saline (vehicle) or IMC-H7 at a dose of 0.3, 1.0 or 3.0 mg/kg (n=4 per group). Body weight and food intake were recorded daily. Five days after the injection period animals were transferred to metabolic cages for 48 hours. This design was then repeated in male hamsters that had been transferred to SD at around 3 months of age and studied at ~6 months of age at which point body weight and adiposity were markedly reduced.

Effect of IMC-H7 treatment on hypothalamic gene expression in relation to body weight, food intake, energy expenditure and substrate utilization

The effects of 3 mg/kg IMC-H7 were measured in age-matched adult male hamsters that had been housed in LD since birth or transferred to SD at ~3 months of age. Animals from each photoperiod were divided into one of two treatment groups and received a single subcutaneous injection of vehicle (saline) or IMC-H7 (3 mg/kg). After 24 hours hamsters were transferred to metabolic cages for the remainder of the study (48 hours). During this time food intake, VO_2 and VCO_2 were measured. At 72h post treatment the animals were euthanized by injection of sodium pentobarbitone (Euthatal: Rhone Merieux, Harlow, UK). Blood samples were collected by cardiac puncture for the determination of circulating hormone concentrations, and the brain for dissected and frozen on dry ice for subsequent analysis of hypothalamic gene expression.

Effects of IMC-H7 treatment in calorically-restricted Siberian hamsters

Five weeks prior to the start of treatment animals were subjected to a restricted food regime. Initially a habituation period was implemented in which hamsters were restricted to just 90% of their individual *ad libitum* food intake for 3 days. Following this initial habituation period individual animal food intake was reduced by a further 10% for a further 3 days, after which, all animals were restricted to 70% of their individual *ad libitum* food intake until an average body weight loss of at least 20% (equivalent to that of SD body weight loss) had been achieved at 5 weeks after the start of the restricted diet regimen. Once pre-determined body loss (~20%) had been achieved all animals were put back on ad libitum food intake and animals were divided into one of two treatment groups (n=6 in each group) in which they received a single subcutaneous injection of either saline or IMC-H7 (3 mg/kg). Food intake and body weight were recorded on a daily basis. Following 72h of the treatment period hamsters were euthanized and the brain was collected for mRNA expression analysis.

Whole-body metabolic analysis

Oxygen consumption (VO_2) and carbon dioxide production (VCO_2) were measured concurrently at 9-min intervals using a modified open circuit calorimeter (Comprehensive Laboratory Animal Monitoring System: CLAMS, Linton Instrumentation, Linton, UK and Columbus Instruments, Columbus, OH) as described previously [S6]. VO_2 and VCO_2 were then used to calculate energy expenditure and the rate of whole body carbohydrate (COX) and fat (FOX) oxidation, as previously described [S7].

In situ hybridization

Briefly, 20μm cryostat sections were fixed in 4% paraformaldehyde in 0.1M-phosphate buffer solution, acetylated in 0.25% acetic anhydride in 0.1M-triethanolamine (pH8). After which, radionucleotide ^{35}S-labeled isotope probes (~10^6 counts/min; table 2.2) were applied to the slides in 70 μl of hybridization buffer containing 0.3 M NaCl, 10 Mm Tris-HCl (Ph 8), 1 Mm EDTA, 0.05% transfer RNA, 10 Mm dithiothreitol, 0.02% polyvinylpyrrolidone, 0.02% BSA, and 10% dextran sulphate. Radionucleotide isotope probes were left to hybridize over night at 55°C. Slides were then washed in a 4 times a sodium citrate solution (1X standard saline citrate = 0.15 M NaCl, 15 mM sodium citrate), treated with ribonuclease A (20 μg/μl) at 37°C and were subsequently washed in 0.1X standard saline citrate solution at 60°C. Finally, radioactive slides were dried and exposed to Biomax autoradiographic MR film together with a ^{14}C microscale for 24h – 7 days depending upon the activity of the radionucleotide isotope probe being used.

Image analysis

Radionucleotide intensity analysis was conducted using Image pro PLUS (version 4.1.00, Media Cybernetics, Wokingham, UK) analysis software. Briefly, autoradiographic films containing recorded images of all experimental slides were scanned at 600dpi on an Umax scanner linked to a PC running

Image pro PLUS. For each radionucleotide probe 3 coronal cross sections spanning the selected region of the hypothalamus were chosen for image analysis. Integrated optical density for each region was obtained by reference to a standard curve generated from the ^{14}C microscale.

microCT: assessment of adiposity
Hamsters were imaged pre-treatment and post-treatment and the changes in adipose tissue volumes determined. Briefly, computed tomographic (CT) imaging of the hamster torso was carried out on Mediso nano-pet/CT under general anesthesia (1.5% isoflurane), using a Helical Tube voltage of 45kVP, exposure 600ms, number of projections 360, pitch 1 and 1:4 binning, pixel 96μm. The image reconstruction was carried out using Ramlak filter, 100% cut off. To quantify the visceral and subcutaneous fat depots, all image analysis was performed with VivoQuant software (inviCRO), 3D regions of interest were drawn using the integrated neighbourhood thresholding tool and Hounsfield unit definition -500 to +200 to give the volume of fat deposition.

Hormone assays
ELISA kits (Millipore, MA, USA) were used to measure circulating levels of insulin (rat/mouse kit EZRMI-13K) and leptin (mouse kit EZML-82K) in plasma samples. Blood glucose was measured using a HemoCue 201 system (Angelholm, Sweden).

Statistical analysis
Descriptive statistics (mean ± SEM) were generated using GraphPad Prism (Prism 6.0, GraphPad, San Diego, CA). Body weight, food intake and CLAMS data were analyzed using a two-way (treatment x sampling time) repeated measures ANOVA, with Bonferroni corrections used as a post-hoc test. Tissue weights, gene expression analysis and protein abundance were analysed using one-way ANOVA or student unpaired t-test where appropriate. Statistical significance was declared at $P<0.05$.

Supplemental References
S1   Ebling, F.J.P. (1994). Photoperiodic differences during development in the dwarf hamsters Phodopus sungorus and Phodopus campbelli. General and comparative endocrinology *95*, 475-482.
S2   Kilkenny, C., Browne, W.J., Cuthill, I.C., Emerson, M., and Altman, D.G. (2010). Improving bioscience research reporting: the ARRIVE guidelines for reporting animal research. PLoS Biology *8*, e1000412. doi:1000410.1001371/journal.pbio.1000412.
S3   Bolborea, M., Helfer, G., Ebling, F.J., and Barrett, P. (2015). Dual signal transduction pathways activated by TSH receptors in rat primary tanycyte cultures. Journal of Molecular Endocrinology *54*, 241-250.
S4   Prevot, V., Cornea, A., Mungenast, A., Smiley, G., and Ojeda, S.R. (2003). Activation of erbB-1 signaling in tanycytes of the median eminence stimulates transforming growth factor beta1 release via prostaglandin E2 production and induces cell plasticity. Journal of Neuroscience *23*, 10622-10632.
S5   Jethwa, P.H., Warner, A., Nilaweera, K.N., Brameld, J.M., Keyte, J.D., Carter, W.G., Bolton, N., Bruggraber, M., Morgan, P.J., Barrett, P., and Ebling, F.J.P. (2007). A VGF-derived peptide, TLQP-21, regulates food intake and body weight in Siberian hamsters. Endocrinology *148*, 4044-4055.
S6   Warner, A., Jethwa, P.H., Wyse, C.A., I'Anson, H., Brameld, J.M., and Ebling, F.J.P. (2010). Effects of photoperiod on daily locomotor activity, energy expenditure and feeding behavior in a seasonal mammal. American Journal of Physiology *298*, R1409-R1416.
S7   Frayn, K.N. (1983). Calculation of substrate oxidation rates in vivo from gaseous exchange. Journal of Applied Physiology *55*, 628-634.
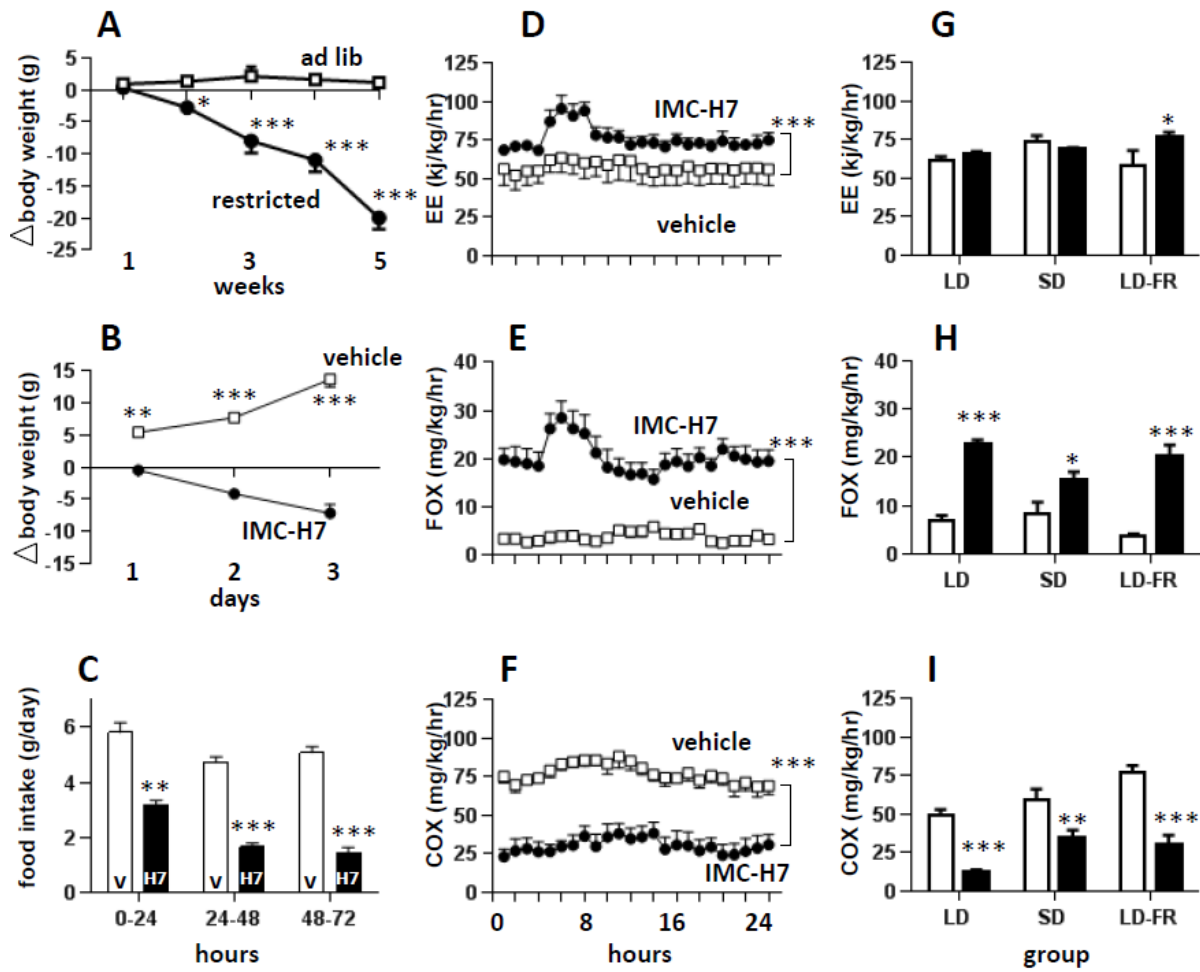
Figure S1
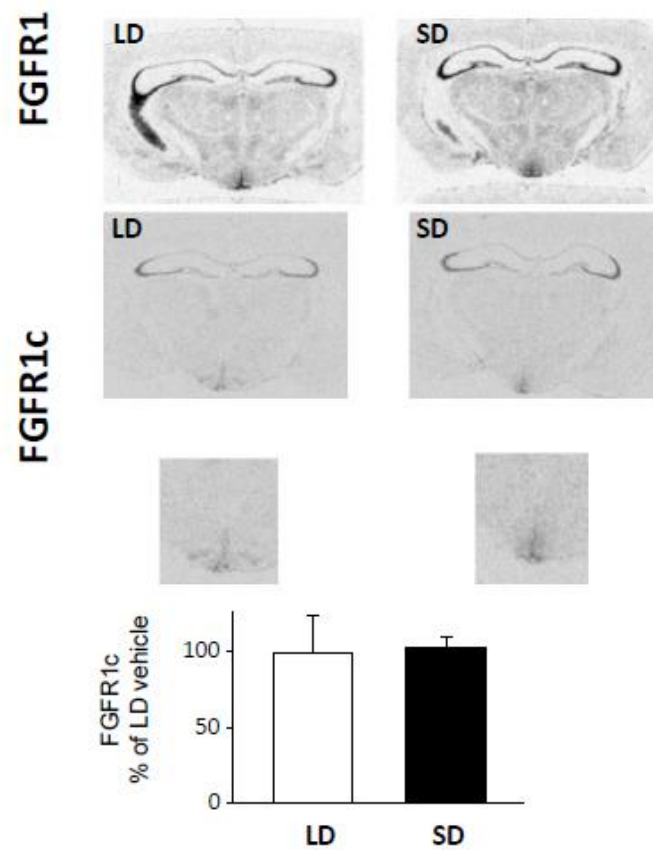
Figure S1, related to Figure 1. Representative autoradiographic images of coronal brain sections from hamsters in long days (LD) or after exposure to short days (SD) depicting hybridization of a FGFR1 probe (**top**) or a FGFR1c-specific probe (**middle**), mediobasal hypothalamic region is expanded below main image. Quantification of the hybridization signal in the mediobasal hypothalamus revealed no effect of photoperiod on signal intensity (**bottom**).
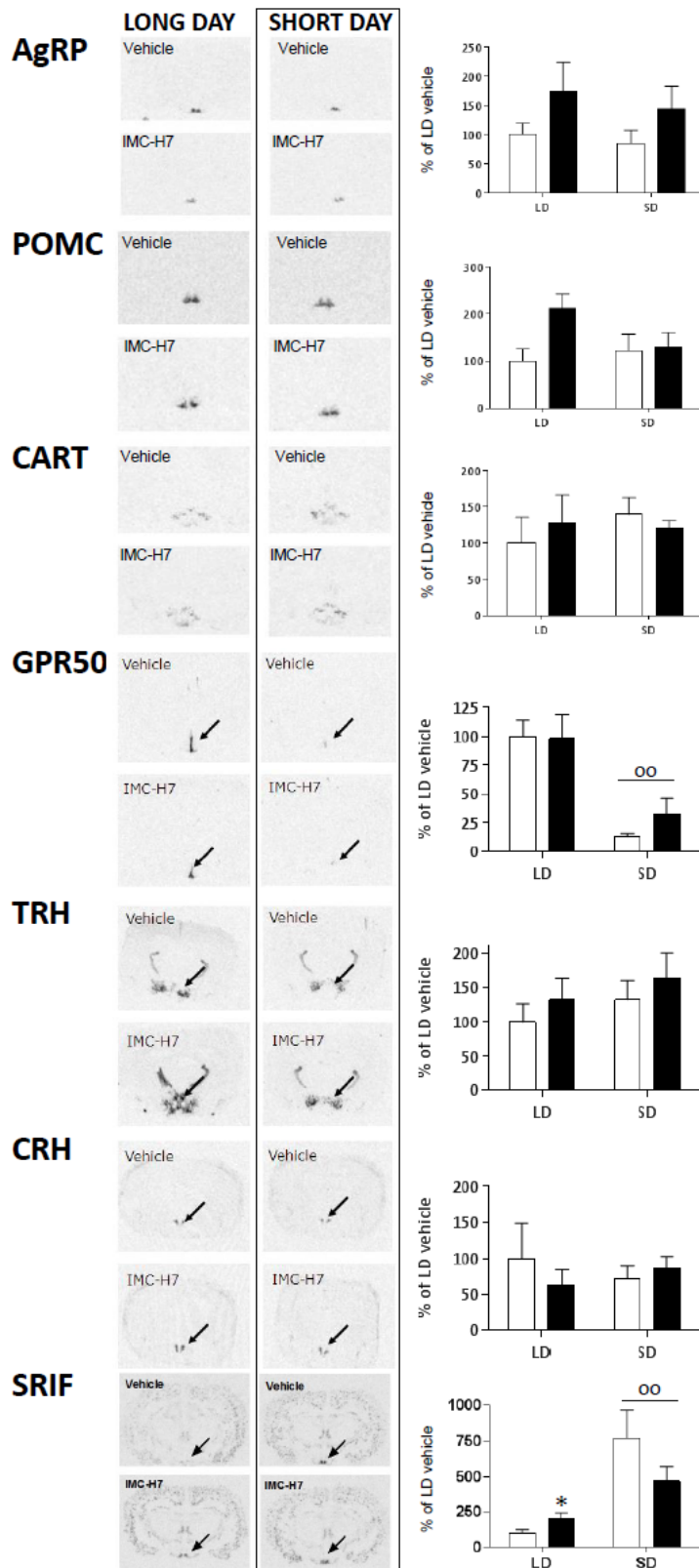
Figure S2
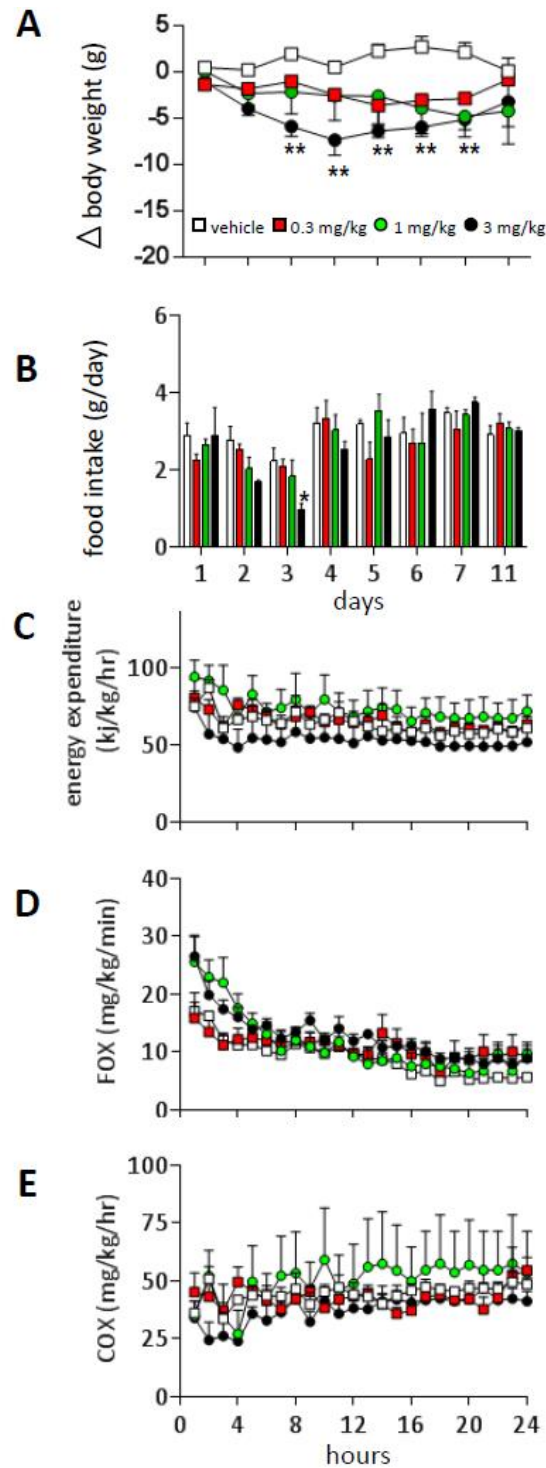
Figure S2, related to Figure 2. **A:** changes in body weight and **B:** daily food intake in adult male hamsters exposed to short days (SD) for 12 weeks and treated subcutaneously with vehicle (□) or increasing doses of IMC-H7 (■ 0.3 mg/kg, ● 1.0 mg/kg, ● 3 mg/kg) and monitored for 11 days, values are group mean ± SEM, n=4 per treatment, **p<0.01 vs vehicle. Hamsters were placed in metabolic cages (CLAMS) 5 days after vehicle or IMC-H7 treatment, values shown are hourly mean ± SEM values calculated for energy expenditure (**C**), fat oxidation (FOX: **D**) and carbohydrate oxidation (COX: **E**) from day 6-7 after treatment.

Figure S3

Figure S3, related to Figure 3. **A:** changes in body weight in adult male hamsters in LD subject to a progressive calorie-restriction protocol (●) or maintain on ad libitum diet (□),*p<0.05, ***p<0.001 vs vehicle. **B:** body weight and **C:** food intake in previously food-restricted hamsters returned to *ad libitum* food after vehicle (□) or IMC-H7 (● 3 mg/kg) treatment, values are group mean ± SEM, n=6 per treatment, **P<0.01, ***p<0.001 vs vehicle. **D-F:** analysis of metabolic cage (CLAMS) data, hamsters were placed in the CLAMS 24 hours after vehicle (c) or IMC-H7 treatment (● 3 mg/kg), values shown are hourly mean ± SEM values for energy expenditure (**C**), fat oxidation (**D**) and carbohydrate oxidation (**E**) from hours 48-72 after treatment, ***p<0.001 vs vehicle. **G-I** 24-hour mean values for these parameters were calculated from the long-day (LD) and short-day (SD) groups in the main photoperiod study (Fig. 2) and for the previously food restricted hamsters in this study (LD-FR), note that the magnitude of the response to IMC-H7 treatment in the LD-FR group more closely resembles that in the LD group than the SD group; *p<0.05, **p<0.01 and ***p<0.001 vs vehicle.

Figure S4, related to Figure 4. **Left:** representative autoradiographic images of coronal sections, and **right:** relative density of signal for hypothalamic genes in adult male hamsters in LD or SD, 7 days after treatment with vehicle (□) or 3 mg/kg IMC-H7 (■). Density values were normalized to LD vehicle, values are group mean ± SEM, n=6 per group. **Top** to **bottom**: agouti-related peptide (AgRP), pro-opiomelanocortin (POMC), cocaine-and-amphetamine-regulated transcript (CART), G protein-coupled receptor 50 (GPR50), thyroid releasing hormone (TRH), corticotropin-releasing hormone (CRF) and somatostain (SRIF). Density analyses were of AgRP and POMC in the arcuate nucleus, CART in the arcuate nucleus and lateral hypothalamus, and TRH and CRH in the paraventricular nucleus. These genes were not significantly affected by photoperiod or FGFR1c blockade. GPR50 was localized to the ependymal cell layer, and was down regulated by SD (°°$P<0.01$ vs LD), but not affected by FGFR1c blockade. SRIF in the arcuate nucleus was significantly increased by IMC-H7 treatment in LD (*$P<0.05$ vs vehicle) and also significantly increased by SD photoperiod (°°$P<0.01$ vs LD).